A Method for Sensorizing Soft Actuators and Its Application to the RBO Hand 2

Vincent Wall Gabriel Zöller Oliver Brock

***Abstract*— The compliance of soft actuators makes manipulation safer and simplifies control. But their high flexibility also makes sensorization challenging. From the large space of possible deformations not all are equally important. We present a method for sensorization of soft actuators that, for a given application, finds an effective layout from a set of sensors. It starts from a redundant sensor layout and iteratively reduces the number of sensors. Applying the method to the PneuFlex actuators of the RBO Hand 2, we identify a layout of four liquid metal strain sensors and one pressure sensor to predict actuator deformation in three dimensions: flexional, lateral, and twist. Finally, the layout is used to build a sensorized RBO Hand 2. It can detect passive shape adaptation while grasping and reveals failure cases during manipulation, e.g. slipping fingers while opening a door.**

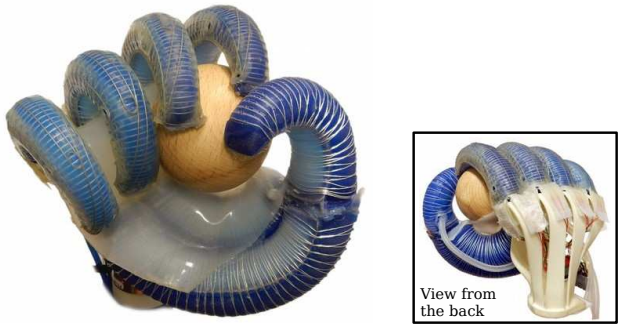

Fig. 1. Using our method we sensorized the RBO Hand 2, enabling detection of deformations that commonly occur during manipulation.

I. Introduction

Soft robotics has had significant impact in a number of areas of robotics, ranging from grasping [1] to locomotion [2]. This impact stems from desirable properties of soft robotic systems: they are inherently safe and, when properly designed, increase robustness to uncertainty while reducing the requirements for perception and control. This is maybe most easily seen in robotic hands, where the use of softness has become the standard design paradigm [1], [3], [4]. When grasping with these hands, their softness lets the hand passively adapt to the shape of the grasped object, without explicit sensing or control.

But there is also a price to pay for softness when it comes to sensing. Due to their ability to deform in many different ways, the configuration of a soft robotic system can only be described accurately with a very large number of parameters. Many sensors would be required to determine all of them. In addition, most traditional sensor technology, e.g. joint and motor encoders [5] or inelastic tactile sensing [6], are not suitable for the integration with soft actuators because of the softness of the materials. At the same time, extrinsic sensing, e.g. through visual tracking [7], [8], limits the field of operation and is susceptible to (self-) occlusions. Still, there is an unbroken need for sensing in soft systems. As we will see in Section IV, even applications particularly well-suited for the soft robotics paradigm still benefit substantially from sensing. Taken together, sensing—and in particular proprioception—remains an open problem in soft robotics.

In this paper we present a method for sensorizing soft actuators. Recognizing the fact that a very large number of sensors would be required to fully reconstruct the shape of the actuator, we propose a method by which we identify the most appropriate placement of sensors, given a number of target deformation modes of particular relevance in a given application. Starting from a redundant sensor configuration, the layout is iteratively reduced to a simpler set of sensors, while minimizing the prediction error.

While the method itself is agnostic to the specific sensor type, we demonstrate it using soft, flexible and stretchable strain sensors that can be integrated into soft actuators without negatively affecting their advantageous properties. We validate the proposed method in the context of grasping with the RBO Hand 2 [1]. Given three deformation modes deemed important for manipulation, we determine an appropriate sensor layout and confirm it in real-world experiments. Our results demonstrate that the method we propose enables the sensorization of soft actuators for applications in which it is not necessary to reconstruct all aspects of deformation.

II. Related Work

The compliance of soft actuators introduces new requirements for the sensor technologies. The sensors need to be as flexible as the actuator to not restrict them. For the human hand several flexible sensors have been developed. They measure contact and bending by means of bi-metallic strips and dielectric stretchable thin-metal films [9], [10]. However, soft actuators often exhibit stretch of more than 200% [1], which these sensors can not achieve. Other flexible sensors based on carbon-infused silicone are capable of greater elongation [11], but exhibit unfavorable time effects due to their viscoelastic material properties.

Recently, the use of liquid metal made it possible to build highly stretchable strain sensors with maximum elongations

All authors are with the Robotics and Biology Laboratory, Technische Universität Berlin, Germany

We gratefully acknowledge financial support by the European Commission (SOMA, H2020-ICT-645599) and by the Alexander von Humboldt foundation and the Federal Ministry of Education and Research (BMBF).

comparable to soft actuators. Metal alloys, like eutectic gallium-indium (EGaIn), are liquid at room temperature and can be used to detect strain through change in resistance. Various patterns have been proposed to sense contact and multi-axial strain using silicone-embedded EGaIn [12]–[15]. These sensors are promising candidates for the integration with soft actuators.

Only very few studies of sensorized soft actuators have been published. Homberg et al. [16] presented a three-fingered pneumatic hand, equipped with commercially available resistive flex sensors. A single sensor in each finger provides feedback about its curvature, which is used to recognize objects during grasping. Bilodeau et al. [17] included liquid metal strain sensors directly into the fabrication process of a pneumatic four-fingered gripper. They use the sensor measurements in conjunction with the actuation pressure to detect if an object was grasped. Farrow and Correll [18] published a design for an easily customizable liquid metal strain sensor. They inject EGaIn into prefabricated silicon tubes for simple and robust manufacturing. Attached to a pneumatic actuator they use the sensor to estimate the diameter of cylindrical objects. All of these solutions use only a single sensor per actuator and can consequently only detect movement in the plane of actuation. However, the key feature of soft actuators is their passive compliance. For this reason most interactions cause deformations in more than one dimension. For many manipulation tasks perception of additional deformation dimensions offers valuable insights about the grasp. Depending on the expected tasks, additional sensing is therefore required.

There have been efforts to create computational methods to optimize sensor placement on soft structures for higher dimensional deformations [19], [20]. These are, however, based on (approximate) actuator models which often are not available. We therefore propose a method that uses experimentally gathered data instead of a model, to identify an effective sensor layout for a given task.

III. Sensorization Method

To be able to fully reconstruct the shape of a soft actuator, a very large number of sensors would be necessary. In many applications, however, the space of relevant deformations is only a subset of all possible deformations. We therefore propose a method to sensorize soft actuators which, given a specific application, finds the most appropriate sensor layout.

This section describes the general process for any soft actuator in six steps. In Section IV the same steps are applied to sensorize the RBO Hand 2.

1) Target Selection: Initially, all application-relevant variations to the actuator's state have to be identified. For many manipulation tasks this will be some form of deformation of the actuator. But any other measurable physical property, e.g. contact location, is permissible. For the grasping application, we chose to sensorize the RBO Hand 2 to detect the deformation modes shown in Fig. 2.

(a) Pulling on a door handle (b) Pushing against a wall (c) Lifting a heavy bottle

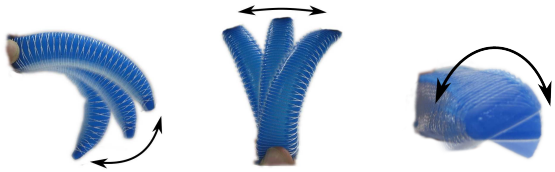

(d) Flexional (e) Lateral (f) Twist

Fig. 2. Deformations during common manipulation tasks: (a) flexional deformation while pulling on a door handle, (b) lateral deformation caused by pushing against a wall, (c) combined twist and lateral deformation while lifting a heavy bottle. (d-f) individual deformation modes

2) Redundant Sensor Layout: Approximate modeling and human intuition is used to generate an initial, redundant layout of sensors for the selected deformations. Through minor variation in the placement of similar sensors redundancy is introduced. Fig. 3 shows the redundant sensor layout that was selected for the PneuFlex actuators of the RBO Hand 2.

3) Obtaining Training Data: In order to perform supervised learning in the next step, labeled training data is required. For this the soft actuator is manipulated in ways that are expected to occur in the envisioned application. Meanwhile the sensor data and ground truth of the target deformation are recorded. Part of the recorded training data is shown in Fig. 4.

4) Supervised Learning: The training data is used to learn a mapping from sensor data to the deformation of the actuator. The choice of learning algorithm depends on the type of target data. The quality of the sensor layout is evaluated with the prediction error of the trained model on an independent validation set. Fig. 5 shows an excerpt of the learned PneuFlex deformation estimation.

5) Layout Reduction: The redundant sensor layout is reduced to find the most appropriate set of sensors for the task. For this a variant of the Recursive Feature Elimination (RFE) algorithm [21] is applied, which excludes the least relevant sensor in each iteration. By using a subset of the already recorded data, no new measurements are needed. The reduction is repeated until only a single sensor is left. Two steps of the applied layout reduction are shown in Fig. 6.

6) Final Layout: The validation error of each intermediate layout during the reduction steps indicates its quality. The sensor layout with the lowest error offers the most accurate mapping of sensor data to deformations. It is chosen as the final layout. Fig. 8 illustrates the resulting layout for the PneuFlex actuator.

IV. Application to the RBO Hand 2

We now apply the proposed method to the RBO Hand 2. It consists of seven highly underactuated, pneumatic actuators, called PneuFlex [1]. During grasping and manipulation they constantly adapt their shape when interacting with object and environment. To perceive these changes sensorization is necessary. The four fingers of the RBO Hand 2 are identical PneuFlex actuators. We use our method to find an effective sensor layout that can detect commonly occurring deformations. (We do not consider the palm and thumb actuators here, as they have different geometries.)

Each step corresponds to the respective step of the sensorization method described in Section III.

1) Target Selection: To determine the relevant deformation we observed the RBO Hand 2 during common manipulation tasks (Fig. 2). From all possible deformations, the following three best describe the actuator state:

- **Flexional:** A displacement in the actuated direction.
- **Lateral:** The finger bends to the side.
- **Twist:** A rotation about the longitudinal axis.

2) Redundant Sensor Layout: Farrow and Correll [18] presented a highly stretchable liquid metal strain sensor that works well with PneuFlex-like actuators. Its thin design has little influence on the actuator's compliance and can easily be adapted to specific sensor shapes. Additionally we measure the air pressure of the actuator. Because this is required for actuation anyway, it adds no further complexity to the setup.

With a proper model of the actuator we could analytically identify good sensor positions. However, for the PneuFlex actuator no reliable information exists on the deformation behavior. Instead we have to create the initial, redundant sensor layout based on intuition and observations. For each deformation mode we observe the path of maximum stretch by studying the rubber hull of the actuator. We then introduce redundancy by placing multiple strain sensors with slight variations along this path. The resulting initial sensor layout (Fig. 3) consists of ten strain sensors: two on the back, three on the sides, and five wrapped around the finger diagonally.

3) Obtaining Training Data: To obtain the ground truth about the actuator shape we use a motion capture system (MoCap) by Motion Analysis. With markers on the base and the fingertip we track the deformation of the actuator in 3D-space. The magnitude of each deformation mode is extracted from the MoCap data by calculating the transformation between the initial resting position of the actuator's fingertip and its current pose in each frame. Flexional deformation is expressed as the angle of the fingertip's rotation in the actuation pane. Lateral deformation is quantified as the offset of the fingertip in millimeters that occurs perpendicular to the actuation pane. Twist is the angle of rotation about the actuators longitudinal axis (base to fingertip).

We use a data acquisition system from LabJack to record the data from the strain and pressure sensors.

We performed the experiment in five identically structured trials. Each trial consists of five different inflation steps. Pressures are selected equidistant from 0 kPa (deflated, straight) to 200 kPa (maximally inflated). We randomized the step order to eliminate the risk of temporal effects. Before each step we perform a calibration movement–one complete inflation and deflation–to account for small sensor offsets caused by unreliable electrical sensor connections.

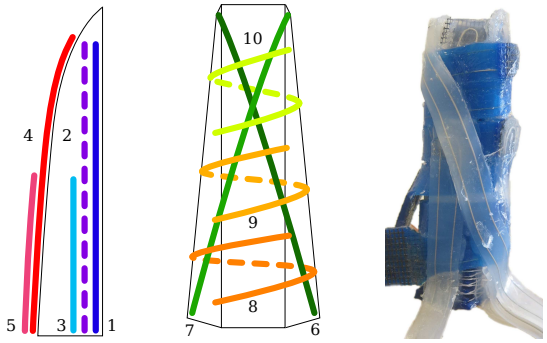

(a) Side View (b) Top View (c) Prototype

Fig. 3. The redundant sensor layout for the PneuFlex actuator (dashed parts hidden by the actuator)—Sensor names: 1–right (full length), 2–left (full length), 3–right (half length), 4–top (full length), 5–top (half length), 6–single twist (ulnar), 7–single twist (radial), 8–multi twist (proximal), 9–multi twist (middle), 10–multi twist (distal)

At each pressure level the actuator is deformed manually by applying forces to the fingertip. The movements are chosen to mimic the deformations observed during grasping experiments. They include both individual and combined occurrences of the three deformation modes.[1]

Fig. 4 shows the recorded data for a single pressure step. Vertical lines indicate calibration, inflation, deformation, and deflation segments. The IDs correspond to those in Fig. 3, with "P" denoting the pressure sensor.

4) Supervised Learning: We apply polynomial regression learning methods from the Scikit-learn toolbox [22] to the recorded training data. Of the five complete trials, one trial is randomly selected as test set. The remaining four trials are used in a leave-one-out cross-validation scheme. The prediction error is determined as the average of the four cross-validation mean squared errors (MSE). Because the best degree of polynomial regression is not known beforehand, we vary it from 1 to 4 and compare the results. Both the full polynomial expansion with all polynomial combinations of features and the *interaction_only* setting, which considers only combinations between different features, are investigated. For brevity we will abbreviate the regression methods using the shorthand XY, where X refers to the polynomial degree and Y denotes "all combinations (A)" or "interaction only (I)", respectively.

Fig. 5 shows the result for a 2I-regression (2^{nd} degree, interactions only). Data from all 11 sensors are used to predict the three deformation modes. The original deformations recorded in the MoCap are plotted in black.

5) Layout Reduction: Our implementation of the RFE algorithm works by comparing n alternative layouts of $n-1$ sensors, where n is the number of sensors at the beginning

[1]Example video available at `https://youtu.be/Rvkl-5AEKLs`

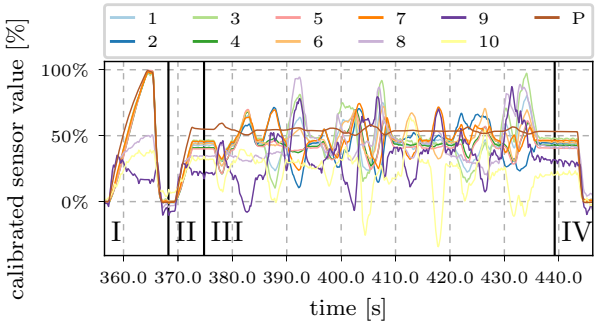

(a) Sensor readings used as training data (Sensor IDs as in Fig. 3)

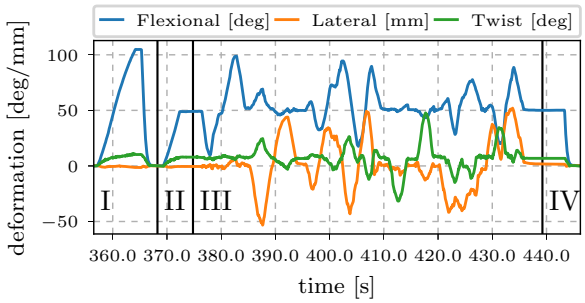

(b) Deformations used as target data

Fig. 4. Training data of a single pressure step (Horizontal segments indicate: I–Calibration, II–Inflation, III–Manual deformation, IV–Deflation)

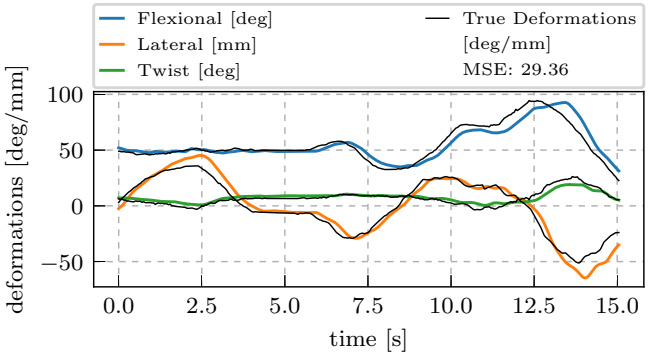

Fig. 5. Deformation estimation using all eleven sensors and a 2I-regression

of each iteration. In each layout one sensor is left out. The layout with the lowest MSE across all regression methods is selected and used in the next iteration. This repeats until only one sensor is left.

Fig. 6 shows the results for the first reduction to five sensors and a later iteration to find the best five-sensor layout. Each column represents one reduced layout, where the label indicates which sensor has been left out. Each row is for a different regression method. The MSE for each layout and algorithm is represented by a colormap. The yellow 'X' highlights the *lowest* MSE and thereby the best combination of regression method and sensor layout. This layout is then used in the next reduction step.

6) Final Layout: The result of the layout reduction is summarized in Fig. 7. For each number of sensors it shows the MSE of the best layout-regression combination. The

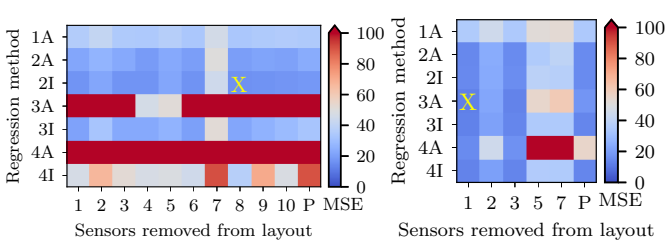

(a) 10-sensor layout reduction (b) 5-sensor layout reduction

Fig. 6. The MSE of each combination of layout and regression method for two feature elimination steps (See text for explanation of labels)

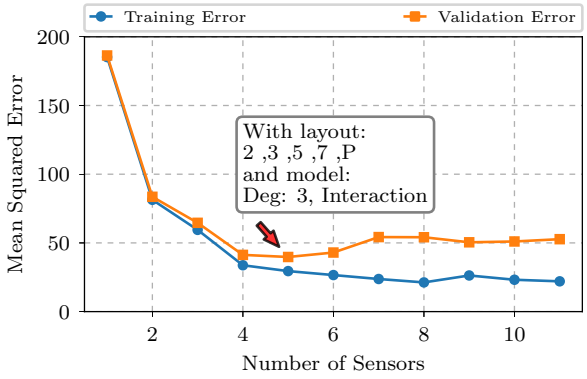

Fig. 7. Validation curve of the sensor layout reduction, highlighting the final combination of layout and model

lowest value across all sensor sets is marked with an arrow. This represents the layout that most effectively predicts the chosen three deformation modes. When using fewer sensors not enough variation in the data can be explained and both training and validation error increase. When using more sensors, however, the divergence of the two errors indicates an over-fitting of the regression to the training data.

The final sensor layout (Fig. 8) chosen by our method for the three deformation modes of the PneuFlex actuator has a total of five sensors: the four strain sensors 2–left (full length), 3–right (half length), 5–top (half length), and 7–single twist (radial), plus the pressure sensor.

V. Evaluation of the Sensorized RBO Hand 2

We sensorized the RBO Hand 2 with the goal of gaining additional insights on interactions during manipulation tasks. To evaluate if the sensorization was able to accomplish that, we use the hand in two example tasks: A compliant grasp of a spherical object and the pulling of a door handle (Fig. 9).

1) Grasping: When grasping an object with the compliant RBO Hand 2 the fingers passively adapt their shapes. This passive deformation should be visible in the deformation data. Fig. 10 shows the estimated deformations during the grasp of a spherical object. Each subplot shows one deformation mode for all four fingers. Three observations are highlighted in the plots:

- **Arrow I:** The index finger has a noticeably larger flexional deformation compared to the other fingers. This indicates that it is not participating in the grasp.

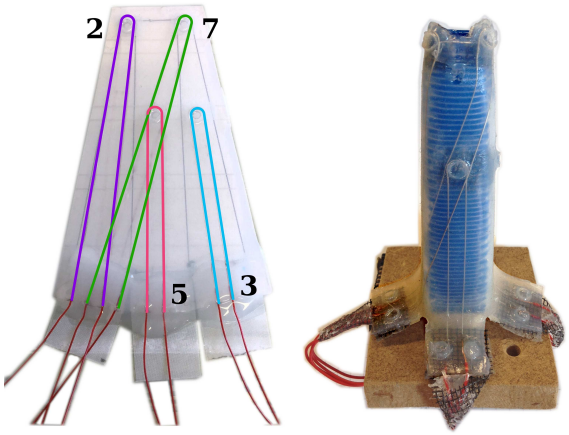

(a) Final sensor layout (b) Sensorized PneuFlex acutator

Fig. 8. The four strain sensors of the final layout are fabricated in a single layer and placed on the PneuFlex actuator. (Sensor IDs as in Fig. 3)

(a) Grasping a sphere (b) Pulling a door handle

Fig. 9. The sensorized RBO Hand 2 is evaluated in two manipulation tasks. Full videos are available in the paper attachment and at `https://youtu.be/H8p4WbFqtgQ`.

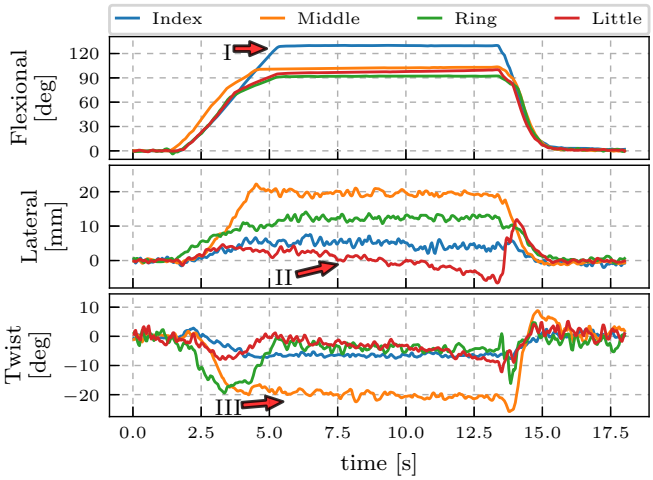

Fig. 10. While grasping a sphere the sensorized RBO Hand 2 estimates the deformation. The three marked observations are discussed in V-.1

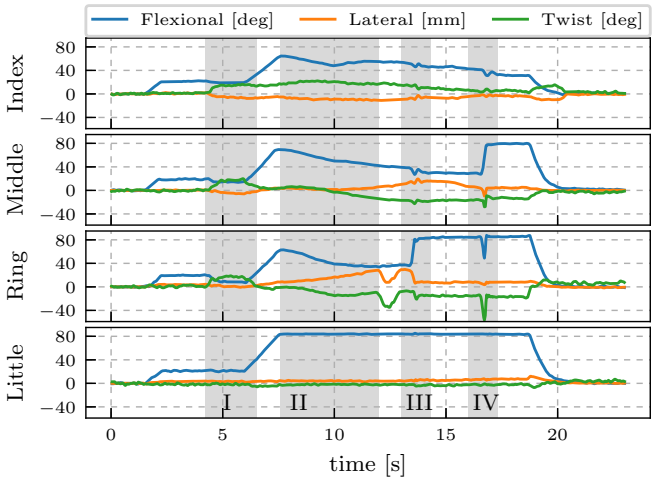

Fig. 11. The deformation of the sensorized RBO Hand 2 is estimated while pulling on a door handle. The four marked sections are discussed in V-.2.

- **Arrow II:** All four fingers show different levels of lateral deformation. The slight slope in the graph of the little finger, however, indicates that the finger is slowly slipping.
- **Arrow III:** The twist of the middle finger can be seen in the last subplot. This is a good example of passively compliant grasping.

2) Pulling: In a second manipulation task we use the sensorized RBO Hand 2 to pull the handle of a door. The soft fingers are not strong enough to hold on to the handle and start to slip. With successful sensorization, the estimated deformations should show the slippage in the flexional component as the fingers bend away and finally slip off the handle. In Fig. 11 each subplot shows the three deformations of one of the four fingers during the task. Four notable situations are highlighted:

- **Situation I:** Three fingers make contact with the door handle. The little finger shows no additional deformation because it misses the handle.
- **Situation II:** The three fingers close around the handle and start pulling. They begin to slip, which can be seen in the decreasing flexional deformation.
- **Situation III:** The middle and ring finger slowly twist away. Then the ring finger slips off the handle. (The temporary drop in lateral deformation and twist of the ring finger at second 12 can be attributed to a pinched-off strain sensor at the fingertip.)
- **Situation IV:** The middle finger also slips off the handle and bumps into the ring finger. Both fingers show sudden deformations.

VI. Discussion

In the ideal case each orthogonal deformation mode would require exactly one separate sensor to detect it. For the three specified deformations in our use case we found a layout that consists of four strain sensors. This indicates that their positions on the actuator are close to ideal. By using even more redundant sensors initially this result could possibly

be improved further. Alternatively a more accurate actuator model will help to make better informed decisions of where to place sensors. However, even highly detailed models will never capture every aspect of physical interaction, so that the proposed method will stay relevant.

For other applications different or additional deformation modes may be relevant, e.g. detecting the location of contact or failure cases like buckling of the actuator due to high loads. With proper feature representation the same sensorization method can be used for many more applications.

While the method itself is hardware-agnostic, one technical issue we encountered were faulty sensor readings due to the error prone connection between the liquid metal core and the required wiring. However, there have been promising advances in the material sciences, investigating for example biphasic metal films [23], that have the potential to resolve theses issues.

VII. Conclusion

The compliance of soft actuators is beneficial in many applications. At the same time, mechanical softness makes sensorization of those actuators challenging. We presented a method for the sensorization of soft actuators that–given a specific set of relevant deformations–identifies a sensor layout to detect these. The method recursively reduces an initially redundant set of sensors, by minimizing the prediction error of the mapping from sensor data to the relevant subset of deformation modes. We apply this method to PneuFlex actuator, used in the RBO hand 2 for grasping. In this application the three main deformation modes of the actuator are: flexional deformation, lateral deformation, and twist. Our method identified a layout consisting of four liquid metal strain sensors and one pressure sensor.

We used the resulting sensorized actuators to build an RBO Hand 2 with four sensorized fingers. In two manipulation tasks we demonstrated the benefit of sensorization: During compliant grasps, the sensorized hand can detect passive object adaptation of the fingers. The sensor data also reveals grasp failures, caused by soft fingers slipping off a door handle. Our results show that it is possible to perform task-relevant sensing with a small number of sensors in soft actuators, even though their inherent deformation space is extremely high-dimensional.

References

[1] R. Deimel and O. Brock, "A novel type of compliant and underactuated robotic hand for dexterous grasping," *The International Journal of Robotics Research*, vol. 35, no. 1-3, pp. 161–185, March 2016.

[2] X. Gong, K. Yang, J. Xie, Y. Wang, P. Kulkarni, A. S. Hobbs, and A. D. Mazzeo, "Rotary Actuators Based on Pneumatically Driven Elastomeric Structures," *Advanced Materials*, vol. 28, no. 34, pp. 7533–7538, Sept. 2016.

[3] M. G. Catalano, G. Grioli, E. Farnioli, A. Serio, C. Piazza, and A. Bicchi, "Adaptive synergies for the design and control of the Pisa/IIT SoftHand," *The International Journal of Robotics Research*, vol. 33, no. 5, pp. 768–782, Apr. 2014.

[4] L. U. Odhner, L. P. Jentoft, M. R. Claffee, N. Corson, Y. Tenzer, R. R. Ma, M. Buehler, R. Kohout, R. D. Howe, and A. M. Dollar, "A compliant, underactuated hand for robust manipulation," *The International Journal of Robotics Research*, vol. 33, no. 5, pp. 736–752, Apr. 2014.

[5] J. Bae, S. Park, J. Park, M. Baeg, D. Kim, and S. Oh, "Development of a low cost anthropomorphic robot hand with high capability," in *IEEE/RSJ International Conference on Intelligent Robots and Systems (IROS)*. IEEE, Oct. 2012, pp. 4776–4782.

[6] M. Lowe, A. King, E. Lovett, and T. Papakostas, "Flexible tactile sensor technology: bringing haptics to life," *Sensor Review*, vol. 24, no. 1, pp. 33–36, 2004.

[7] Y. Shapiro, A. Wolf, and K. Gabor, "Bi-bellows: Pneumatic bending actuator," *Sensors and Actuators A: Physical*, vol. 167, no. 2, pp. 484–494, June 2011.

[8] A. D. Marchese, K. Komorowski, C. D. Onal, and D. Rus, "Design and control of a soft and continuously deformable 2d robotic manipulation system," in *IEEE International Conference on Robotics and Automation (ICRA)*, May 2014, pp. 2189–2196.

[9] G. D. Kessler, L. F. Hodges, and N. Walker, "Evaluation of the cyberglove as a whole-hand input device," *ACM Trans. Comput.-Hum. Interact.*, vol. 2, no. 4, pp. 263–283, Dec. 1995.

[10] A. P. Gerratt, H. O. Michaud, and S. P. Lacour, "Elastomeric Electronic Skin for Prosthetic Tactile Sensation," *Advanced Functional Materials*, pp. 2287–2295, Mar. 2015.

[11] M. Weigel, T. Lu, G. Bailly, A. Oulasvirta, C. Majidi, and J. Steimle, "iSkin: Flexible, Stretchable and Visually Customizable On-Body Touch Sensors for Mobile Computing," in *Proceedings of the 33rd Annual ACM Conference on Human Factors in Computing Systems*, ser. CHI '15. New York, NY, USA: ACM, 2015, pp. 2991–3000.

[12] Y.-L. Park, C. Majidi, R. Kramer, P. Bérard, and R. J. Wood, "Hyperelastic pressure sensing with a liquid-embedded elastomer," *Journal of Micromechanics and Microengineering*, vol. 20, no. 12, p. 125029, Dec. 2010.

[13] Y.-L. Park, B.-R. Chen, and R. J. Wood, "Design and Fabrication of Soft Artificial Skin Using Embedded Microchannels and Liquid Conductors," *IEEE Sensors Journal*, vol. 12, no. 8, pp. 2711–2718, Aug. 2012.

[14] J. W. Boley, E. L. White, G. T.-C. Chiu, and R. K. Kramer, "Direct Writing of Gallium-Indium Alloy for Stretchable Electronics," *Advanced Functional Materials*, vol. 24, no. 23, pp. 3501–3507, 2014.

[15] T. Lu, L. Finkenauer, J. Wissman, and C. Majidi, "Rapid Prototyping for Soft-Matter Electronics," *Advanced Functional Materials*, vol. 24, no. 22, pp. 3351–3356, June 2014.

[16] B. S. Homberg, R. K. Katzschmann, M. R. Dogar, and D. Rus, "Haptic Identification of Objects Using a Modular Soft Robotic Gripper," in *IEEE/RSJ International Conference on Intelligent Robots and Systems (IROS)*. IEEE, 2015, pp. 1698–1705.

[17] R. A. Bilodeau, E. L. White, and R. K. Kramer, "Monolithic fabrication of sensors and actuators in a soft robotic gripper," in *IEEE/RSJ International Conference on Intelligent Robots and Systems (IROS)*, Sept. 2015, pp. 2324–2329.

[18] N. Farrow and N. Correll, "A soft pneumatic actuator that can sense grasp and touch," in *IEEE/RSJ International Conference on Intelligent Robots and Systems (IROS)*, Sept. 2015, pp. 2317–2323.

[19] U. Culha, S. G. Nurzaman, F. Clemens, and F. Iida, "SVAS3: Strain Vector Aided Sensorization of Soft Structures," *Sensors*, vol. 14, no. 7, pp. 12 748–12 770, July 2014.

[20] M. Bächer, B. Hepp, F. Pece, P. G. Kry, B. Bickel, B. Thomaszewski, and O. Hilliges, "Defsense: Computational design of customized deformable input devices," in *Proceedings of the 2016 CHI Conference on Human Factors in Computing Systems*. ACM, 2016, pp. 3806–3816.

[21] I. Guyon, J. Weston, S. Barnhill, and V. Vapnik, "Gene selection for cancer classification using support vector machines," *Machine learning*, vol. 46, no. 1-3, pp. 389–422, 2002.

[22] F. Pedregosa, G. Varoquaux, A. Gramfort, V. Michel, B. Thirion, O. Grisel, M. Blondel, P. Prettenhofer, R. Weiss, V. Dubourg, J. Vanderplas, A. Passos, D. Cournapeau, M. Brucher, M. Perrot, and E. Duchesnay, "Scikit-learn: Machine learning in Python," *Journal of Machine Learning Research*, vol. 12, pp. 2825–2830, 2011.

[23] A. Hirsch, H. O. Michaud, A. P. Gerratt, S. de Mulatier, and S. P. Lacour, "Intrinsically stretchable biphasic (solid–liquid) thin metal films," *Advanced Materials*, vol. 28, no. 22, pp. 4507–4512, June 2016.